Test of neural network techniques using simulated dual-band data of LEO satellites

Anthony V. Dentamaro
Boston College

Phan D. Dao[1]
Kimberly R. Knobel
Air Force Research Laboratory, Space Vehicles Directorate

ABSTRACT

Dual-band, multi-pass simulations of low Earth orbit (LEO) satellites are used to train a feedforward neural network to recognize different classes of resident space objects (RSO). Simulated data allow for a controllable and diverse set of inputs necessary to test our methods, especially at the initial phase of the evaluation, while avoiding the problems and expense associated with real data collection from ground-based facilities. Simulation software is used to generate signatures in two visible bands for satellites exhibiting typical bus-types, materials combinations and methods of stabilization. Orbits and observational parameters are generated from the relevant statistical distribution of the orbital parameters obtained from the Space Surveillance Network, and stabilization is simulated external to the framework of the software used to calculate signatures. We examine various pre-processing schemes that combine temporal, spectral and solar phase angle (SPA) information from non-glinting signatures into vectors that can be used as inputs for our classifier. A metric that assigns a proxy signal-to-noise ratio to each neural network output is introduced to determine the confidence level of each result.

[1] Correspondence author

1. INTRODUCTION

The US Space Command, through the Space Surveillance Network (SSN), has the critical mission of monitoring the health of our space assets and maintaining the catalog of space objects. In addition to the metric data, used for constructing orbital information, photometric and radiometric data is also used for space object identification (SOI). Neural networks have been seen to be one of the suitable tools for SOI in cases where resolved images of satellites are unavailable[1]. Neural networks have been evaluated as a potential automated technique for identifying satellites in geosynchronous Earth orbit (GEO), where only non-resolved signatures are available. Deep space assets are regularly visible, often for long periods of time which allows for the collection of many light curves. Many GEO sats are three-axis stabilized, which means that the crafts reveal almost no relative motion with respect to the observer, and combined with a slowly-varying solar inclination angle, provides the observer with a repeatable set of viewing angles and lighting conditions for each pass. Simulated multispectral light curves of deep-space satellites also provide a good basis for the training and testing of neural networks and are valuable when data from these relatively dim objects are not available[2]. In that paper, attitude control and solar panel articulation are modeled to account for the changing orientation of GEO spacecrafts. The addition of multi-wavelength data to the neural network aids in identification of non-resolved objects by exploiting spectral signatures from the various spacecraft materials[3].

In this work, we employ neural network techniques in the identification of objects in low Earth orbit (LEO) using simulated dual-band spectral data. As spacecraft become smaller, they become more difficult to resolve because of their smaller angular extent, and classifier techniques become valuable tool for SOI. Collection of LEO satellite data presents its own set of challenges for use in evaluating neural networks. To properly evaluate a neural network, multiple photometric measurements must be made for each satellite under similar observational conditions. At the same time, this set of conditions must allow each satellite to be observed over as wide a range of viewing and lighting scenarios as possible. This is complicated by the fact that most LEO satellites are rarely visible from one particular site on a regular basis under typical experimental conditions. Specifically, 1) the satellite must be sufficiently high in elevation to minimize atmospheric effects on the data, 2) for observation in visible wavelengths, the object must not be in eclipse during the pass, and 3) nighttime conditions must exist at the observation sites during collection times. Also to be considered during data collection campaigns are limitations imposed by weather

Report Documentation Page

Form Approved
OMB No. 0704-0188

1. REPORT DATE	2. REPORT TYPE	3. DATES COVERED
SEP 2010		**00-00-2010 to 00-00-2010**

4. TITLE AND SUBTITLE	5a. CONTRACT NUMBER
Test of neural network techniques using simulated dual-band data of LEO satellites	5b. GRANT NUMBER
	5c. PROGRAM ELEMENT NUMBER
6. AUTHOR(S)	5d. PROJECT NUMBER
	5e. TASK NUMBER
	5f. WORK UNIT NUMBER
7. PERFORMING ORGANIZATION NAME(S) AND ADDRESS(ES) **Air Force Research Laboratory,Space Vehicles Directorate,Kirtland AFB,NM,87117-5776**	8. PERFORMING ORGANIZATION REPORT NUMBER
9. SPONSORING/MONITORING AGENCY NAME(S) AND ADDRESS(ES)	10. SPONSOR/MONITOR'S ACRONYM(S)
	11. SPONSOR/MONITOR'S REPORT NUMBER(S)

12. DISTRIBUTION/AVAILABILITY STATEMENT
Approved for public release; distribution unlimited

13. SUPPLEMENTARY NOTES
2010 Advanced Maui Optical and Space Surveillance Technologies Conference, 14-17 Sep, Maui, HI.

14. ABSTRACT
Dual-band, multi-pass simulations of low Earth orbit (LEO) satellites are used to train a feedforward neural network to recognize different classes of resident space objects (RSO). Simulated data allow for a controllable and diverse set of inputs necessary to test our methods, especially at the initial phase of the evaluation, while avoiding the problems and expense associated with real data collection from ground-based facilities. Simulation software is used to generate signatures in two visible bands for satellites exhibiting typical bus-types, materials combinations and methods of stabilization. Orbits and observational parameters are generated from the relevant statistical distribution of the orbital parameters obtained from the Space Surveillance Network, and stabilization is simulated external to the framework of the software used to calculate signatures. We examine various pre-processing schemes that combine temporal, spectral and solar phase angle (SPA) information from non-glinting signatures into vectors that can be used as inputs for our classifier. A metric that assigns a proxy signal-to-noise ratio to each neural network output is introduced to determine the confidence level of each result.

15. SUBJECT TERMS

16. SECURITY CLASSIFICATION OF:			17. LIMITATION OF ABSTRACT	18. NUMBER OF PAGES	19a. NAME OF RESPONSIBLE PERSON
a. REPORT **unclassified**	b. ABSTRACT **unclassified**	c. THIS PAGE **unclassified**	**Same as Report (SAR)**	**10**	

or otherwise poor seeing conditions. Given these considerations, it could take many campaigns, based at several different sites, to collect the requisite amount of data. Certainly, it is preferable to have actual data, and future data collection campaigns are planned, but simulations are used in this phase to immediately test the viability of the method.

2. SATELLITE MODELS

Optical Signatures Code (OSC) was developed by Teledyne Solutions, Inc. for U.S. Army Space and Missile Defense Command. It is a set of programs that, among other functions, models ballistic and satellite trajectories and calculates infrared and visible optical signatures of hardbodies. Several simulation packages exist that would be appropriate for this study, but we use OSC for these tests because of ready access to the source code and our ability to use the software to readily model specific spacecraft. Wireframe models of satellites are constructed from a palette of shapes available to the user. The number of shapes, as well as the number of facets available on each shape, can be modified to allow more complete representations of space objects and increased accuracy in the calculation of self- obscuration and self-shadowing of the models. Typical materials are assumed for the surfaces, based on information that can be found for each satellite. Reflectance is assumed to be primarily Lambertian , plus a small (20%) specular component to allow for glinting surfaces, such as solar panels. Radiant intensities are calculated for a blue band (468-495 nm) and a red band (738-765 nm). Active satellites are used, which require that attitude control be accurately maintained. For this set of experiments, we externally control the orbit propagation and the satellite's attitude and feed OSC with the relevant parameters needed for the generation of the radiant intensity.

Table 1 lists the set of six satellites used in this work. Several criteria were used to select the objects. All satellites are active so that attitude-control can be imposed. Satellites all execute low Earth orbits with inclination angles in the 35-65 degree range, thus making neural network identification dependent only on satellite geometry and spectral signature, presenting a more rigorous test for the neural network. The revisitation rate, or frequency with which a satellite is seen from a ground-based platform under typical experimental conditions, must be high enough to generate enough light curves to conduct the tests. Revisitation rate is increased by increasing the number of observation sites. Table 2 lists four facilities from which we have received or taken data in past collaborations and are chosen for our simulations. In addition to solar illumination and nighttime operation (solar declination greater than 10 degress) requirements, we impose the condition that objects must rise to an elevation of at least 20 degrees to be considered visible from a site. No more than one spacecraft is used from any satellite constellation, with the exception that satellites from two different generations of the Orbcomm constellation are chosen because they are in very similar orbits but are structurally different, providing an example of a case where satellites can be cross-tagged. Fig. 1 shows solid body representations of the OSC wireframe satellite models which were constructed using the WinOSC GUI included in the OSC software package.

Table 1. List of Simulated Satellites

Satellite Name	Country	SSN Number	Inclination	Purpose	No. of Obs
FalconSat 3	US	30776	35.432	Civil/Mil	28
TecSAR	Israel	32476	41.026	Mil	20
Orbcomm FM20	US	25416	44.998	Com	41
Orbcomm Q2	US	33060	48.444	Com	34
LatinSat B	Argentina	27606	64.558	Com	42
Jason 1	US/France	26997	66.043	Gov	95

Orbital position is generated from the relevant statistical distribution of the orbital parameters obtained from the Space Surveillance Network. Orbits are propagated using a MATLAB code ported from Vallado's C codes of SPG4 by Jeff Beck [4,5], and modified for vector operations. Resulting altitudes, latitudes and longitudes are compared to values posted in a real-time satellite tracking website[6]. Agreement to within 0.01 degrees in latitude and longitude and ~100 meters in altitude were obtained. Sun position and the position of the observers are also generated as a function of time in the Earth-Centered, Earth-Fixed (ECEF) frame for input to OSC.

Table 2. Observation Sites

Site Name	Location	Latitude (N)	Longitude (E)	Altitude (m)
Hanscom AFB	Bedford, MA	42.49	288.72	122
MRO	Socorro, NM	33.99	252.81	3193
AMOS	Maui, HI	20.70	203.72	3058
NOFS	Flagstaff, AZ	35.58	248.59	2273

A typical stabilization mode is simulated by generating nine direction cosines for each time interval, which describe the orientation of the body axes in ECEF frame. Nadir-aligned, Velocity-constrained (NAVC) stabilization is used, where the main body axis (Z_B) of the satellite points toward Earth center and the velocity is constrained to the X_B direction. Each satellite in this study possesses an antenna that points toward the Earth, so NAVC stabilization is suitable for the bodies of the six satellites studied here. Limiting the scope of this work to active satellites serves two purposes; a realistic situation is presented by a satellite of known stabilization, and the resulting simulated data can be used in future classification techniques and characterization schemes where deactivated objects are either not interesting or not useful. A list of active satellites can be found in many places on the Internet, such as a database compiled by the Union of Concerned Scientists[7] which is updated every two weeks.

Ground-based observation points, as are used here, require long simulated observational periods to accumulate the required number of data points. Orbits were propagated through 100,000 5-sec time steps, which simulates an approximately six-day observation period, starting at the epoch time of the TLE used for each satellite. When a satellite is visible for at least one of the observation sites, OSC is used to calculate radiant intensity in the blue and red spectral bands, taking into account obscuration and shadowing and optical properties of the surfaces. After all the OSC runs are completed, the outputs are prepared in a format for input to the neural network. The last column of Table 2 indicates how many total times each satellite is seen (number of light curves collected) over the course of the observation period. Files which do not provide enough data to generate a useful light curve are discarded.

3. NEURAL NETWORK AND PRE-PROCESSING OF DATA

Neural networks can be valuable tools for the type of pattern recognition problem posed by non-resolved SOI from light curves. The behavior of the neural network is defined by the way its individual computing elements are connected and by the strengths of these connections, or weights. The weights are automatically adjusted by training the network according to a specified learning rule until it performs the task correctly. Supervised learning is used because each light curve used for training is associated with a specific satellite. The MATLAB Neural Network Toolbox supports different types of networks, so the architecture is customized to fit our requirements. Pattern recognition problems, such as SOI, are best approached using a feedforward neural network in which weights are only updated after all the inputs and targets are presented. Backpropagation is the learning rule which is useful when the network is trained with one set of data and is tested with a different, non-overlapping data set. For this first test, the default setting of one hidden layer consisting of 20 neurons is used. Backpropagation requires that the transfer function, which calculates a scalar output from the weighted input vectors, be differentiable, so we use the default tan-sigmoid function. As a result, the values of the output nodes are compressed to lie between 0 and 1. Training is commenced using the default value of 1000 epochs, or number of times the entire training set is fed forward through the network. The number of epochs is increased until the success rate, or percentage of time a light curve is correctly identified, is seen to stabilize. No significant improvement in identification is seen for more than 3000 epochs.

Different schemes are considered to prepare, or pre-process, the data to assist the neural network in its identification. Light curves are presented to the neural network in the vector form

$$LC_j = [a_{j1}, a_{j2}, a_{j3}\ldots\ldots\ldots a_{jn}],$$

where n is the number of input nodes for each input light curve LC_j. Input node, a_{ji}, contains the i*th* value of radiant intensity for the j*th* pass of a satellite. In this work, the n input nodes are values of radiant intensity in one spectral band, or a linear combination of the signal from the red and blue bands, calculated for a specific solar phase angle (SPA).

Fig. 2 shows sample light curves for each of the six satellites pre-processed by two different schemes. The red lines plot the integrated radiant intensity in the red band (738-765 nm) as a function of SPA, while the blue line represents the spectral difference, B-R, of the signal in the two bands. It is seen that for LEO objects, SPA values can vary widely from one observed pass to the next. In order to present the data to the neural network under consistent conditions, a pre-selected range that is common to as many passes as possible is chosen. Radiometric data for a wide sample of lighting and observing conditions is desirable, but not always practical. About 120 light curves are generated in our simulations in which the satellites are observed for a minimum interval of 30 degrees in SPA, but not always for the exactly same range in each case. Approximately one-third of these files include data that span the entire SPA range of 70-100 degrees. A significant number of files contain data for 30 degree intervals that either start or end in the 70-100 degree range, but do not include radiant intensity values for the entire set of SPA angles. Visual examination of the plots of the data using different pre-processing schemes reveals that for any one particular satellite, the light curve profiles do not appear to vary significantly by shifting the center of the SPA range by up to $\pm$15 degrees. We use data sets that fit this criterion to increase the number of inputs available for training and testing. In the next section, the effect that this shift in SPA has on the results is examined.

An interpolation algorithm is used to generate 61 values of radiant intensity at 0.5 degree resolution for each data set. Preliminary tests confirm that results improve with training, so approximately half of the available data sets are used to train the network, with the rest reserved for testing. Six output modes, one for each satellite, are activated as a result of the testing procedure. A measure of the success rate for identification is given by the number of most strongly-activated output nodes which are associated with the correct satellite.

4. RESULTS

Neural network results are obtained using single band and spectral-difference light curves. Each plot in Fig. 3 shows the neural network results for testing the red band light curves for one satellite. The fraction of light curves most strongly associated with each of the six satellites is indicated by the height of the corresponding column. All of the light curves for satellites 25416 (Orbcomm FM38), 27606 (LatinSat B) and 30776 (FalconSat 3) are correctly identified, and satellites 26997 (Jason-1) and 33060 (Orbcomm Q2) each have at least a 83.3% success rate. By far, the fewest amount of data sets was available for TecSAR (32476), so the neural network received the least training for this satellite, and the results in this case are the least successful. The test is repeated using the blue band data, with no significant change in the confusion matrix. Approximately 90% of the single band light curves used for testing are associated with the correct satellite. The success rate for the dual-band data is approximately 80%. The neural network is run again for both pre-processing methods, but this time only with data that spans the entire 70-100 degree SPA range. Ten curves from each object are still used for training, (five, for satellite 32476). This test yields 90% and 82% success rates for single-band and dual-band testing, respectively, suggesting that the latitude that was taken with the SPA range does not have a significant effect on the results.

While the brightness data used in our test appeared to provide the neural network with the type of information that can be used to make its identifications, the utility of color indices in aiding SOI is documented[8] and needs to be considered. Combinations of object shape, surface materials and pose give rise to features in one type of data that are not present in another. A metric is needed to evaluate neural network results which performs well for all situations. We start with a closer examination of the results obtained thus far.

Table 3. Neural network weights for the testing of two red band light curves (046 and 047) of Orbcomm Q2 (33060)

LC Tested	**25416**	**26997**	**27606**	**30776**	**32476**	**33060**	***pSNR***
33060 #046	6.72E-05	0.001144	4.82E-14	6.89E-05	0.00515	0.998222	**>500.**
33060 #047	0.038362	5.34E-07	0.145408	0.208011	0.000835	0.011697	**3.79**

Table 3 shows the results from testing two sets of single-band radiometric data from passes of Orbcomm Q2 (33060). Curve 046 records a correct identification because the node associated with 33060 is the most strongly-activated, while Curve 047 is more strongly associated with FalconSat 3 (30776) and LatinSat B (27606). Although the metric indicates a success rate of 50% for these two tests, we assert that the identification for Curve 047 is not as strong as that for Curve 046 and should not be treated equally. A metric is proposed that combines neural network results obtained from both brightness and spectral considerations. The network is run for both single-band and dual-band pre-processing of the data. An algorithm is constructed that:

- reads a the line of output weights corresponding to the test of light curve 1 using single-band results
- calculates a relative strength, $S_{1,sb}$, to the highest weight in the line
- compares $S_{1,sb}$ to threshold T
- if $S_{1,sb} > T$, a positive identification is recorded for light curve 1
- if $S_{1,sb} < T$, the value $S_{1,db}$ is calculated for the test of light curve 1 using dual-band results
    - if $S_{1,db} > T$, the identification is confirmed for light curve 1
    - if $S_{1,db} < T$, light curve 1 cannot be confidently associated with any of the satellites
- repeat with light curve 2, 3,….n

Since each sample contains only six points (the six output nodes), fitting a distribution to the results is not appropriate. Instead, we define the relative strength of an identification as a proxy "signal-to-noise ratio" (pSNR):

$$\mathrm{pSNR} = \frac{\max(\mathrm{a1}, \mathrm{a2}, \ldots . \mathrm{an})}{\sigma(\mathrm{ai} \neq \mathrm{maximum})}$$

where max (a1, a2,….an) = ak is the weight with the highest magnitude, and σ(ai ≠ maximum) is the standard deviation of all values, except for that associated with the most strongly-activated node,

$$\sigma = \sqrt{\frac{\Sigma(\mathrm{ai} - \mu)^2}{\mathrm{n} - 1}}$$

where μ is the mean of the non-maximum weights, and the summation is taken over all i ≠ k. Calculation of pSNR for the identification of the two 33060 light curves is seen in the last column of Table 3. The results show the identification of the #047 curve is indeed much weaker than that of its counterpart and needs to be validated.

A value for the threshold can be estimated by examining the results of all the SNR calculations. The three lowest values of SNR for the single-band testing are clustered together in the interval between 3.79 and 4.22. The next lowest value of SNR ~ 7. This observation is used to set the threshold at pSNR ~ 4.3. Of the three identifications with sub-threshold pSNR, two are attached to incorrect results. So, in the limited sample size of this test, a false positive is returned on the order of 50% of the time when pSNR < threshold. A similar sampling of the pSNR values for the B-R results yields a threshold of 5.5. Table 4 shows the results of the three sub-threshold single-band data sets. It is seen that using our metric confirms one correct result (25416), corrects another result (33060) and is unable to correct one other (26997). So, the net result of combining the neural network outputs for the six satellites is a small increase in the success rate.

Table 4. Comparison of single- and dual- band results for three specific light curves

	Red Band	**B-R**
Sat# / LC# tested	**NN ID / *pSNR***	**NN ID / *pSNR***
25416 / 018	25416 / *3.96*	25416 / *6.81*
33060 / 047	30776 / *3.79*	33060 / *10.74*
26997 / 064	32476 / *4.23*	33060 / *36286.*

Single band pre-processing works well for the six satellite case used in this study, but may not be as effective when resolving the signatures of two or more satellites which are physically similar or are in similar orbits. The efficacy of combining neural network results has already been suggested above. A more extreme example is to examine the case of two sets of identically-shaped satellites in similar orbits. The two Orbcomm satellites (25416, 33060) used earlier are re-modeled using different, but typical, spacecraft materials and propagated through their orbits. The light curves from the two original satellites, plus those from the two modified satellites (25416*, 33060*), are prepared using single- and dual- band methods and fed to the neural network.

Fig. 4 compares the results. For the single-band case, satellites 33060 and 33060* are confused almost as frequently as they are correctly identified, indicating that they are clearly cross-tagged. Dual-band network results completely resolve the two 33060 satellites, and correctly identifies the four satellites for 29 of the 30 test curves. Values of pSNR are calculated for each test using the red data and the B-R data, and threshold values are determined for both cases. Results are then combined and evaluated as they were for the six satellite case. This time, the combination yields an overall identification that improves upon the single-band predictions, but is less than the B-R totals. This is due to the fact that some red band light curves are misidentified with a confidence level much higher than threshold, so the spectral results are not allowed to correct the errors.

5. CONCLUSIONS

A feedforward neural network is tested to identify space objects in low-Earth orbit using simulated dual-band satellite data. High-fidelity wireframe models of six LEO satellites, typical observational conditions and active attitude-control are employed to evaluate the neural network performance. Radiometric signatures collected in a single spectral band under nearly constant lighting and viewing conditions are associated with satellites at a success rate of >90%.

The objective is to construct a metric that allows the neural network to perform well over a variety of scenarios. An algorithm is introduced that calculates a level of confidence for each result as a measure of the goodness of the identification. When the algorithm determines that the value of a proxy signal-to-noise ratio (pSNR) for a single-band result is below an established threshold, the dual-band output is sampled to validate the identification of the light curve. The use of this metric is also applied to the case of identically-shaped objects with different materials sets, and the inclusion of color is seen to be important in resolving a possible cross-tagging. In this case, it is the dual-band processing that is more accurate. Overall, the combination of methods yields results that improve upon using either method separately.

The work presented herein represents a first iteration of our methods. More data collection, simulated and real, are planned for future experiments. Additional spacecraft also need to be included to determine the efficacy of these methods and to examine the ability of neural networks to be a viable tool in RSO identification.

6. REFERENCES

1. Cauquy, M.-A.A., Roggemann, M.C. and Schulz, T.J., *Distance-based and neural-net-based approaches for classifying satellites using spectral measurements*, Opt. Eng. **45**(3), 036201, 2006.
2. Poelman, C.J. and Meltzer, S.R., *Spacecraft Identification by Multispectral Signature Analysis Using Neural Networks*, Phillips Laboratory Technical Report PL-TR-97-1053, 1997.
3. Payne, T.E., Sanchez, D.J., Gregory, S.A., Finkner ,L.G., Caudill, E., Payne, D.M., Kann, L. and Davis, C.K., *Color Photometry of GEO Satellites*, Proc. 1999 Space Control Conference, MIT/LL, Lexington, MA, 1999.
4. Vallado, D.A., Crawford, P., Hujsak, R. and Kelso, T.S., *Revisiting Spacetrack Report #3*, AIAA 2006-6753, Proc. of AIAA/AAS Astrodynamics Specialist Conference, Keystone, CO, 2006.
5. www.centerforspace.com/downloads/files/sgp4/AIAA-2006-6753Code.zip
6. http://www.n2yo.com
7. http://www.ucsusa.org/nuclear_weapons_and_global_security/space_weapons/technical_issues/ucs-satellite-database.html
8. Luu, K.K., Snodgrass, J., Sabol, C., Lambert, J., Hamada, K. and Giffin, S.M., *Systematic Effects in Color Photometry Data*, Proc. 2002 AMOS Technical Conference, Maui, HI, 2002.

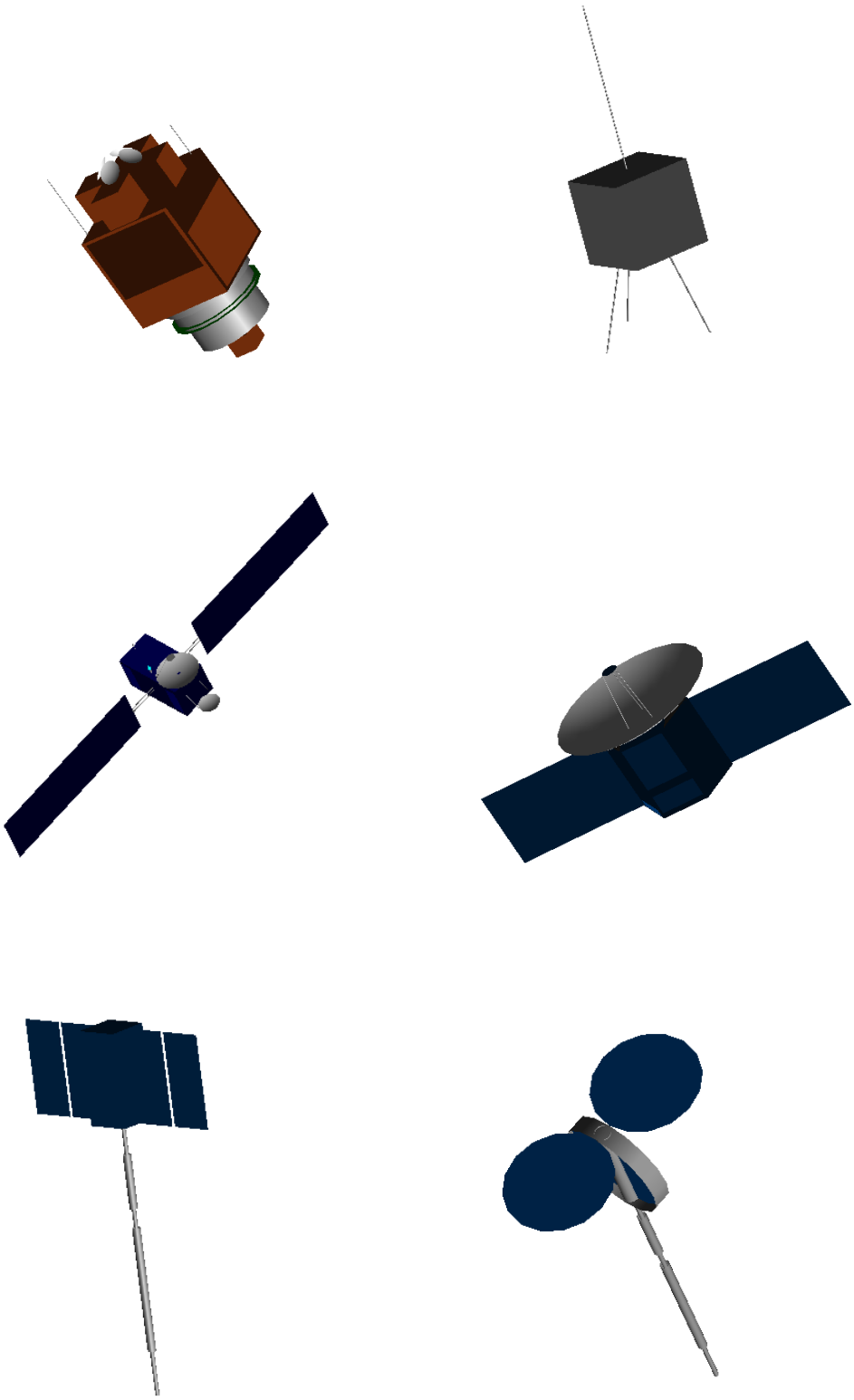

Fig. 1 OSC Solid Satellite Models. Models were constructed using the WinOSC GUI. Clockwise from upper left: FalconSat3, LatinSat B, TecSAR, Orbcomm FM20, Orbcomm Q2, Jason-1.

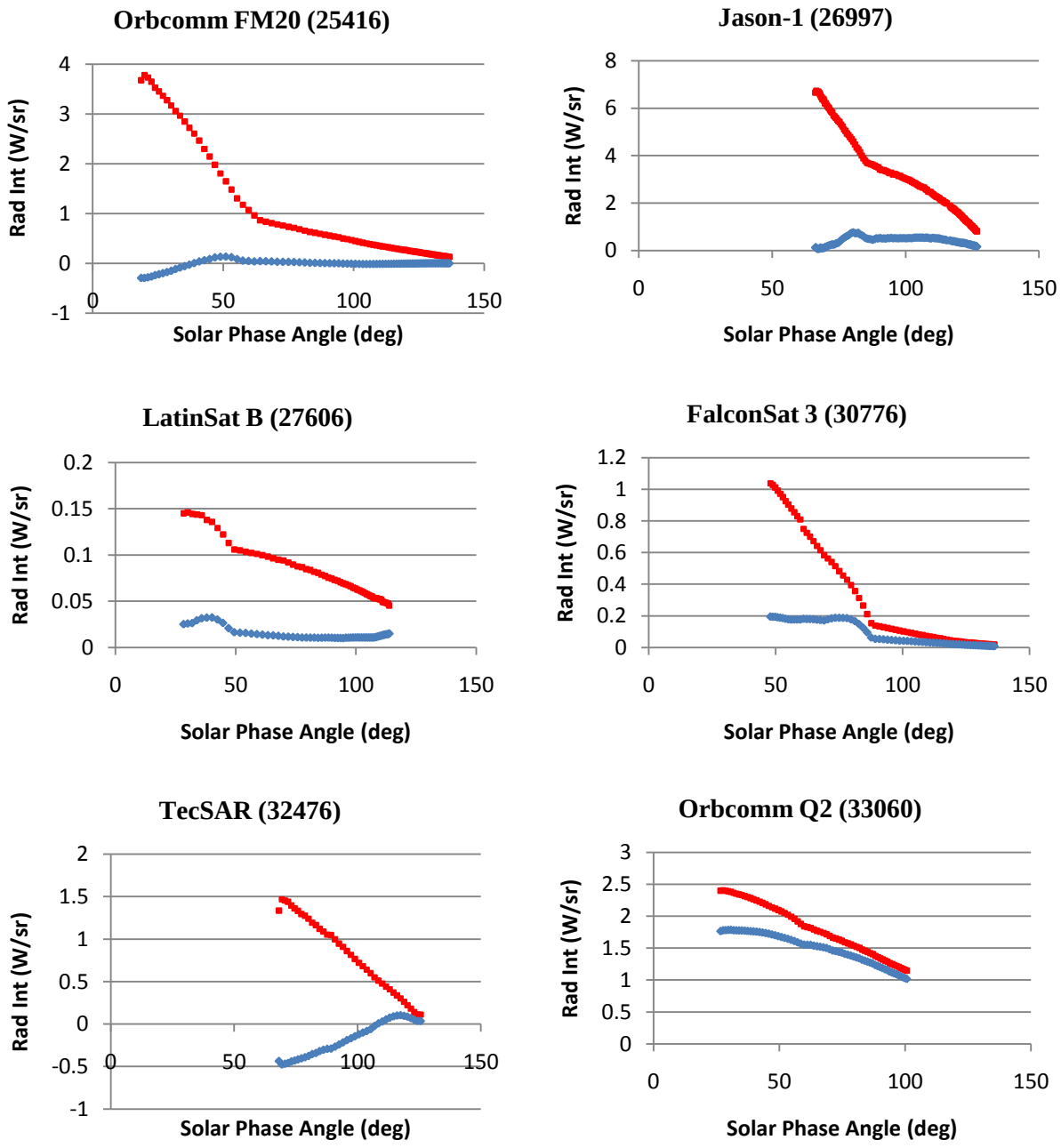

Fig. 2 Sample light curves for each satellite. Red band intensity (red line) and spectral difference, B-R, (blue line) are plotted as a function of SPA. Only light curves with data in the approximate SPA range 70-100 degrees are used to train and test the neural network.

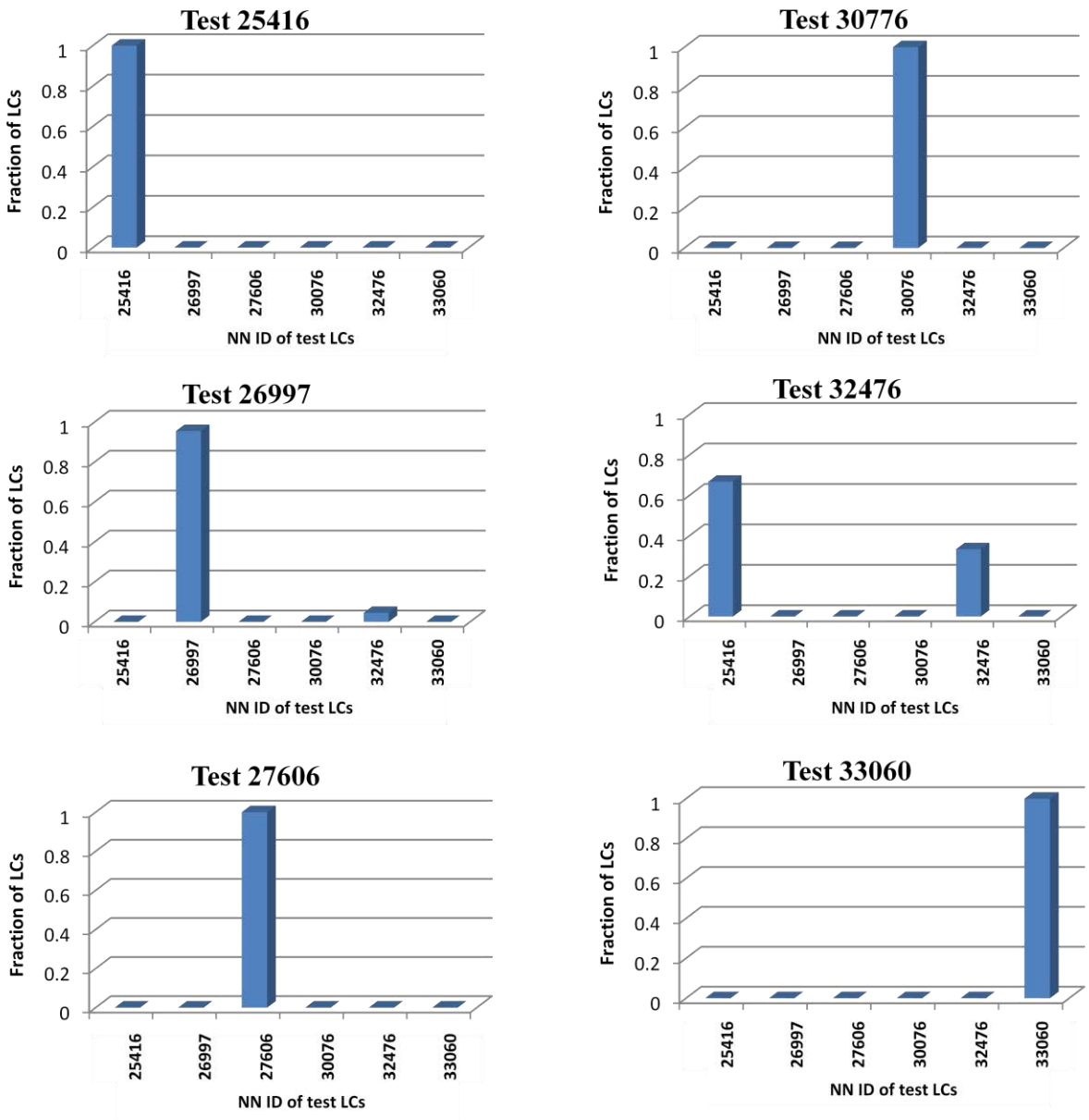

Fig. 3 Neural network identification of space objects. Each plot shows the fraction of tested single band light curves that the network associates with each satellite. Ten curves from each satellite (five from 32476) are used for training. An overall success rate of 92% is recorded.

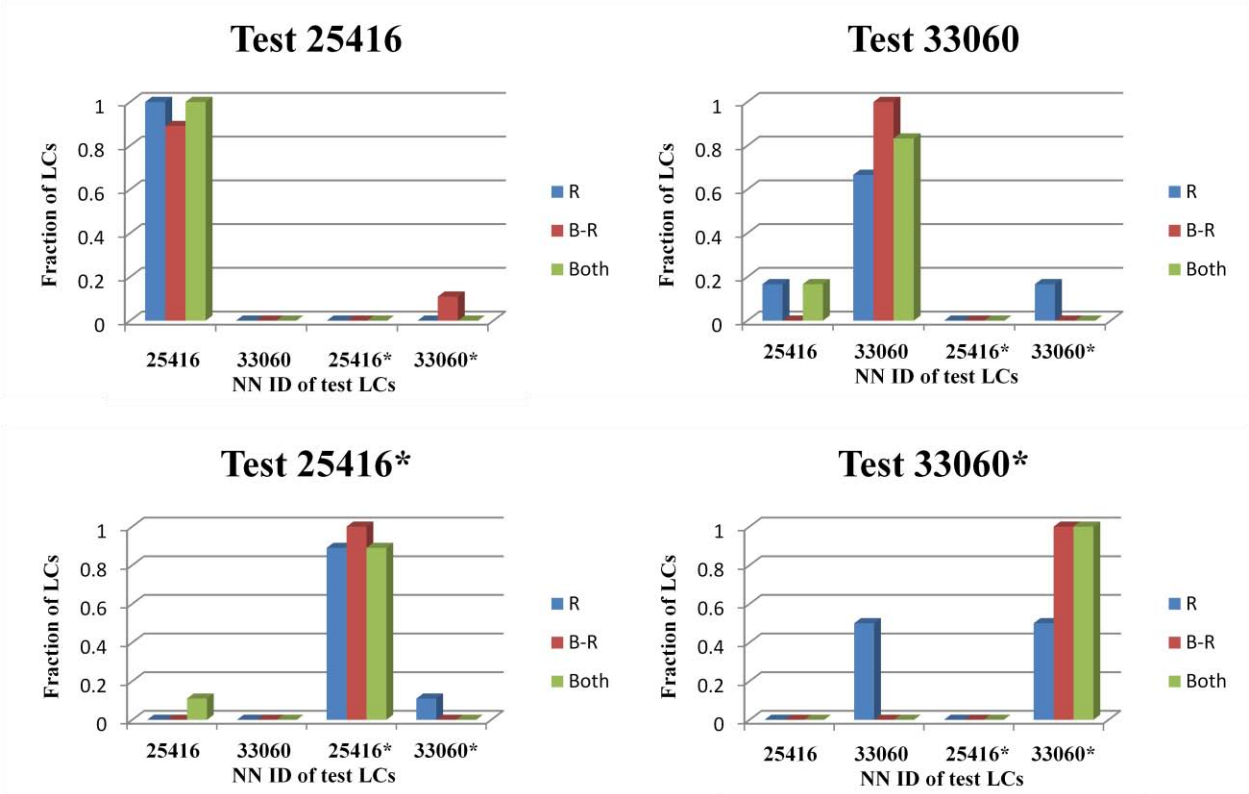

Fig. 4 Neural network results for two sets of identical satellites. Blue column graphs plot the fraction of light curves associated with each object when red band data is used for pre-processing. Red columns indicate the use of dual-band data. Green columns indicate the final results using the SNR metric.